COMMUNICATION

Synergistically activated dual-locked fluorescent probes to monitor H_2S-induced DNA damage

Received 00th January 20xx,
Accepted 00th January 20xx

DOI: 10.1039/x0xx00000x

Yafu Wang, [a,†] Xiaoli Zhao, [a,†] Yuehua Chen, [a] Tony D. James, [a,c] Ge Wang, [b] Hua Zhang [a,*]

Naphthalimide-based fluorescent probes (NAN0-N_3 and NAN6-N_3) were developed with dual locked fluorescence. Significantly, the use of different linkers enabled the probes to adopt different conformations, resulting in changes in the energy dissipation of the excited states, respectively. Where, ≥ 1.9×10^{-2} mM of H_2S and ≥ 2.2×10^{-2} μg/mL of DNA could unlock a highly sensitive off-on fluorescence response through synergistic changes of the molecular structure and conformation. As such the probes could monitor DNA damage induced by the overexpression of H_2S, and were able to evaluate the degree apoptosis of living cells mediated by H_2S-induced mtDNA or nDNA damage.

As a typical endogenous gaseous transmitter, H_2S can regulate the redox equilibrium during oxidative stress.[1] In addition, H_2S participates in DNA damage and repair, and it has a vital role in the DNA damage response (DDR).[2] When H_2S is overexpressed in cells, it affects the cellular antioxidant system, where autooxidation and trace metal-mediated Fenton reaction results in abundant reactive oxygen species (ROS),[3,4] which leads to intracellular redox imbalance and DNA damage. When compared with nuclear DNA (nDNA), mitochondrial DNA (mtDNA) is more susceptible to H_2S, resulting in irreversible and severe damage,[5] because it is located in ROS-producing regions and lacks histone protection.[6,7] H_2S-induced DNA damage results in mutagenic or carcinogenic effects, and seriously accelerates the progression of malignant diseases.[5,6] For example, promoting the breaking of DNA strands and the development of cancer.[7] Therefore, it is essential to devise a suitable tool for monitoring H_2S-induced DNA damage, which is not only beneficial to the study of DNA repair and damage pathways induced by H_2S, but also of great significance for the diagnosis and treatment of DNA-related diseases.

Fluorescent probes are typically composed of a fluorophore, linker, and recognition group. They have been used as effective tools for the visual monitoring of H_2S[8-11] and DNA[12-15] in living cells. For example, an off-on probe with symmetric structure and dual recognition sites has been developed for H_2S that exhibits a low detection limit (2.0×10^{-5} mM) by using -N_3 as the recognition group in a bis-naphthalimide.[8] While a 7-nitro-1,2,3-benoxadizolid has been used as the recognition group to construct a H_2S-specific fluorescent probe, which could detect H_2S down to 2.5×10^{-3} mM in cells.[10] In addition, we have used thread like probes based on dicyanoisoflurone as the fluorophore to specifically bind mtDNA at 7.1×10^{-2} μg/mL generating a highly sensitive fluorescence response due to the inhibition of intramolecular torsion.[12] These previous systems exhibit excellent detection and monitoring ability based on different kinds of fluorescence signal changes. To date, most research has focused on structural modification of the fluorophore and recognition groups and has ignored the importance of the linker. However, a series of G4-DNA specific fluorescent probes were synthesized containing linkers with varying lengths (-$(CH_2)_3$-, -$(CH_2)_2O(CH_2)_2$-, -$CH_2(CH_2OCH_2)_2CH_2$-). Under the synergistic action of the fluorophore and the linker, the probes exist in a folded form, which quenches the fluorescence. After binding with G4-DNA, the conformation of the probes were altered and the fluorescence signal was turned on.[13] Based on the intramolecular dimerization-caused quenching (DCQ) strategy, a series of DCQ probes were constructed using different linkers (lysine, PEG8) and two squaraine units, the probes are quenched in aqueous media. Then when bound to the receptor, molecular conformational changes result in fluorescence turn on.[16] In addition, the triphenylamine and imidazole recognition unit were linked by a short linker (ie. single bond), causing intramolecular torsion, resulting in fluorescence quenching. Thus, when bound to mtDNA G4, the intramolecular torsion was restricted, and the fluorescence was turned on.[17] Inspired by these systems we developed a fluorophore, linker and recognition group system, where the fluorescence is quenched by dual-locking, and can only be turned on by the dual-activation by H_2S reaction and DNA binding. As such, our system enables the detection of H_2S-induced DNA damage.

The fluorophore and DNA specific binding unit was a bis-naphthalimide.[18] Two diamines with different lengths (0-carbon, 6-carbon) were introduced into the bis-naphthalimide structure as linkers. Thus, when the probes bind with DNA, the molecular conformations are changed which removed the fluorescence quenching caused by intramolecular torsion (**NAN0-N_3**) or DCQ (**NAN6-N_3**). This represents a lock, which is specifically opened by DNA binding. Moreover, a fluorescence quenching group -N_3, as a specific recognition group for H_2S, was introduced into both ends of the bis-naphthalimide structure. This further reduces the energy of radiative transitions, and acts as a lock for the fluorescence of the probe, which can be selectively opened using H_2S. The design of these two locks acts as double insurance for quenching of the fluorescence and results in a highly sensitive off-on fluorescence

[a] *Key Laboratory of Green Chemical Media and Reactions, Ministry of Education; Collaborative Innovation Centre of Henan Province for Green Manufacturing of Fine Chemicals; Henan Key Laboratory of Organic Functional Molecule and Drug Innovation; School of Chemistry and Chemical Engineering Institution, Henan Normal University, Xinxiang 453007, China.* zhanghua1106@163.com
[b] *School of Basic Medical Sciences, Xinxiang Medical University, Xinxiang 453007, China.*
[c] *Department of Chemistry, University of Bath, Bath, BA2 7AY, UK.*
† *Yafu Wang and Xiaoli Zhao contributed equally to this work.*
† Footnotes relating to the title and/or authors should appear here.
Electronic Supplementary Information (ESI) available: [details of any supplementary information available should be included here]. See DOI: 10.1039/x0xx00000x

response when both locks are opened using the two keys H_2S and DNA, facilitating the detection of H_2S-induced DNA damage. The specific synthetic route (**Fig. S1**) and structural characterization of the two probes (**NAN0-N_3**, **NAN6-N_3**) are given in the **Supporting Information**.

Firstly, the recognition ability of **NAN0-N_3** and **NAN6-N_3** (6.7 μM) for H_2S or/and DNA were verified. **NAN0-N_3** and **NAN6-N_3** generated spectral changes, controlled by changes in the conformation and structure. As shown in **Fig. 1** and **S2**, **NAN0-N_3** and **NAN6-N_3** were non-fluorescent in the free state. While **ND-N_3** (2-carbon) was used as a model probe whose initial fluorescence was negligible (**Fig. S3**).[8] The different linkers, result in different conformations in the free state. **NAN0-N_3** (0-carbon) with shorter linker exists in the torsional form (**NAN0-N_3(T)**, **Fig. 2**), while **NAN6-N_3** (6-carbon) exists in the folded form (**NAN6-N_3(F)**, **Fig. 2**), which greatly reduces the energy of radiative transitions, *i.e.* fluorescence quenching (first lock).[16,17,19] When H_2S was added, the absorption of **NAN0-N_3** at 375 nm decreased, and a new absorption signal appears at 495 nm which gradually increases with increasing H_2S (**Fig. S2a**). The same result was obtained for the absorption spectra of **NAN6-N_3** (**Fig. S2b**). In addition, the new peaks (m/z[M+Na]: 445.1064) and (m/z[M+Na]: 515.3523) appeared in the HRMS spectra with the addition of H_2S, respectively. It confirms that H_2S causes a change of structure from **NAN0-N_3** (m/z[M+3H]: 477.1438) or **NAN6-N_3** (m/z[M+Na+2H]: 569.3312) to **NAN0-NH_2** or **NAN6-NH_2** (**Fig. S17**). However, the fluorescence intensities of these molecules (**NAN0-NH_2** and **NAN6-NH_2**) were only slightly larger than those of **NAN0-N_3** and **NAN6-N_3** (1.1 fold **Fig. S2c** and **S2d**), indicating that they are still quenched. This is because **NAN0-NH_2** and **NAN6-NH_2** are still in a torsional conformation (**NAN0-NH_2(T), Fig. S4**) or folded conformation (**NAN6-NH_2(F), Fig. S4**), even though their molecular structures have changed (**Fig. S4**). Yet, for the same process, the fluorescence of **ND-N_3** was significantly enhanced with increasing H_2S. Significantly, there was no observed fluorescence enhancement for **ND-N_3** with DNA (**Fig. S3**).[8] This is because there is no conformational change for **ND-N_3** only a structural change after reaction with H_2S.

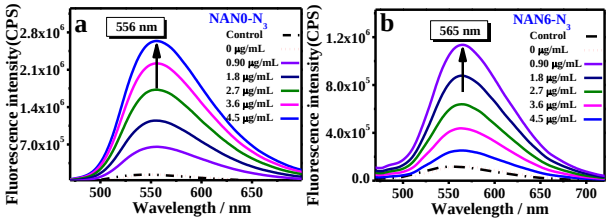

Fig. 1. The response of **NAN0-N_3** and **NAN6-N_3** (6.7 μM) towards DNA and H_2S in tris-HCl (0.05 M, pH = 7.4, 37 °C). a and b, The emission spectra of **NAN0-N_3** (a, λ_{ex} = 425 nm) and **NAN6-N_3** (b, λ_{ex} = 410 nm) towards DNA (0-4.5 μg/mL) in the presence of Na_2S (3.3 mM). Black dotted line (Control): probe (6.7 μM); Red dotted line (0 μg/mL): probe (6.7 μM) and 3.3 mM Na_2S. Na_2S solution (0.1 M) was used as H_2S releasing agent. Commercial smDNA was used for this experiment.

Furthermore, the absorption spectra of **NAN0-N_3** (**Fig. S2e**) and **NAN6-N_3** (**Fig. S2f**) exhibit no change when DNA was added. That is, the addition of DNA has no effect on the molecular structure of **NAN0-N_3** and **NAN6-N_3** (**Fig. S5**). The molecular docking results of **NAN0-N_3** and **NAN6-N_3** with DNA (**Fig. S5**) indicated that **NAN0-N_3** (binding energy = -70.06 kcal/mol) and **NAN6-N_3** (binding energy = -88.18 kcal/mol) are bound to DNA through minor groove interactions, resulting in conformation changes and transformation into **NAN0-N_3(I)** and **NAN6-N_3(I)** (**Fig. S5**), respectively. As such, the torsion of **NAN0-N_3(I)** was restricted and stacked **NAN6-N_3(I)** was unfolded (**Fig. S5**). These changes decreased the energy of the non-radiative transition, however, the sensitive fluorescence turn on was still inhibited by the -N_3 (*i.e.* the second lock) of **NAN0-N_3(I)** and **NAN6-N_3(I)**. However, with an increase of DNA, the fluorescence of **NAN0-N_3** (**Fig. S2g**) and **NAN6-N_3** (**Fig. S2h**) exhibited a weak enhancement. These results indicated that the probes could respond to H_2S or DNA, but only generated a weak fluorescence response due to a single key (recognition factor) being used with these dual locked systems.

NAN6-N_3 exhibited a good linear response for the targets (**Fig. 1** and **Fig. S6**). And a highly sensitive fluorescence output could be activated with ≥ 2.7×10^{-2} mM H_2S and ≥ 8.2×10^{-2} μg/mL DNA coexisting in the test system. In addition, **NAN0-N_3** could be activated to generate a highly sensitive fluorescence signal in the presence ≥ 1.9×10^{-2} mM H_2S and ≥ 2.2×10^{-2} μg/mL DNA (**Fig. 1** and **S6**). Significantly, the lowest concentrations of H_2S that could activate the probes were higher than the normal expression range for H_2S in cells, however higher levels associated with over expression could activate the probes.[20,21] These spectral results are because probes (**NAN0-N_3(T)** and **NAN6-N_3(F)**) underwent conformational changes (**NAN0-N_3(I)** and **NAN0-N_3(I)**) after binding to DNA, which reduced the energy dissipation in the excited state. In addition, H_2S reduces the -N_3 to -NH_2 (**NAN0-NH_2(T)** and **NAN0-NH_2(F)**), and the intramolecular electron cloud density increased. Therefore, under the synergistic action of conformational and structural changes (**NAN0-NH_2(I)**, **NAN6-NH_2(I)**), a highly sensitive fluorescence signal was generated (**Fig. 2**). That is, **NAN0-N_3** and **NAN6-N_3** could be activated by H_2S and DNA in solution. And importantly, this response could be used for the detection of DNA damage induced through the overexpression of H_2S in cells.

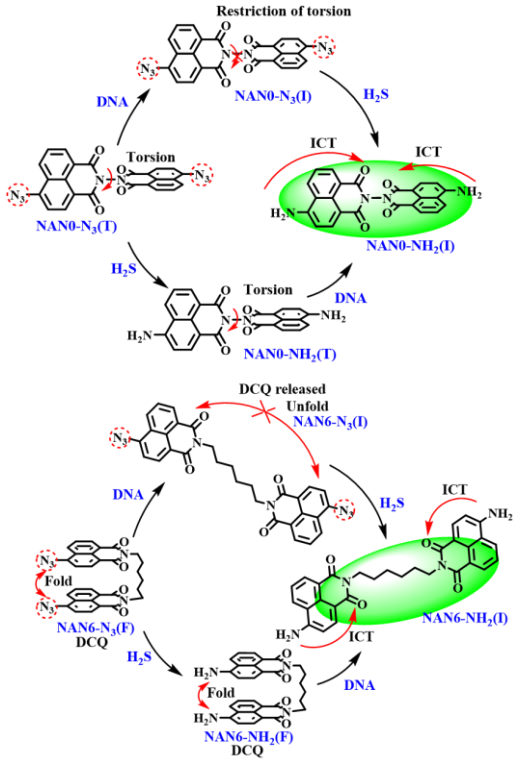

Fig. 2. The response mechanism of **NAN0-N_3** and **NAN6-N_3** to H_2S and DNA.

Fig. S7-S10 verified that **NAN0-N_3** and **NAN6-N_3** exhibited good biocompatibility, which was conducive to the specific monitoring of H_2S-induced DNA damage in cells. To verify the specific binding ability of **NAN0-N_3** and **NAN6-N_3** for DNA in cells, HepG2 cells were pretreated with different concentrations of DNA digesting enzymes (0, 50.0 and 100.0 U/mL) for 1.0 h. These results (**Fig. S11**) indicated that all the probes (6.0 μM) exhibited fluorescence in the green channel (535-575 nm). In addition, as the concentration of DNA digestive enzymes increased, DNA damage was enhanced and the fluorescence intensity of **NAN0-N_3** and **NAN6-N_3** decreased significantly. That

is, **NAN0-N_3** and **NAN6-N_3** could only bind with intact DNA in cells, while DNA binding altered the molecular conformation, which reduced the fluorescence quenching caused by intramolecular torsion (**NAN0-N_3**) or DCQ (**NAN6-N_3**), and resulted in the fluorescence being partially turned on. These results are consistent with those from the solution-based experiments (**Fig. S2**). In addition, when HepG2 cells were pretreated with 1.0 mM PAG (DL-Propargylglycine, an inhibitor of cystathionine γ-lyase during endogenous H_2S synthesis) for 1.0 h,[10] their fluorescence intensity remained constant (**Fig. S12**). That is, normal levels of H_2S expressed in live cells cannot reduce -N_3 (one of the locks) to -NH_2, and the fluorescence remains in a semi-quenched state. In contrast, the fluorescence of **ND-N_3** did not change after the addition of DNA digestive enzyme, and decreased significantly with treatment by PAG, indicating that **ND-N_3** exhibits no response to DNA and its fluorescence signal was only influenced by H_2S.

In addition, the stained areas of living cells using these probes were significantly different. The commercial mitochondrial dye (Mito-Tracker Deep Red) and nuclear dye (Hoechst 33258) were used as standard localization dyes in HepG2 cells to investigate the localization, respectively. As shown in **Fig. S13**, the Pearson's correlation coefficient (Rr) for the staining region of **NAN6-N_3** (6.0 μM), Hoechst 33258 (10.0 μM) and Mito-Tracker Deep Red (5.0 μM) were 0.37, 0.96, respectively, which indicated that **NAN6-N_3** could accumulate in the DNA of the mitochondria, *i.e.* mtDNA. Furthermore, the region stained by **NAN0-N_3** overlapped with that for Hoechst 33258 (10.0 μM, Rr = 0.91), suggesting that **NAN0-N_3** could enter the nucleus and specifically detect nDNA. That is, the different length of the linkers could regulate the flexibility, biological activity and lipophilicity of the probes, thus realizing the accumulation in different subcellular regions of the cell. These imaging results confirmed that **NAN0-N_3** and **NAN6-N_3** could achieve specific binding with nDNA and mtDNA, respectively.

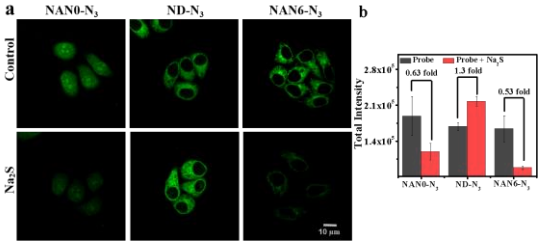

Fig. 3. Imaging of H_2S-induced DNA damage in HepG2 cells. a, The imaging of H_2S-induced DNA damage in HepG2 cells. HepG2 cells were pretreated with Na_2S to establish H_2S-induced DNA damage cell model. Stained with **NAN0-N_3**, **ND-N_3** and **NAN6-N_3** (6.0 μM), respectively. Excitation wavelength = 405 nm, scan range = 535-575 nm (green channel). Incubation time: 30.0 min. b, Histogram of the green channel in (a). Fold: intensity final / intensity at start.

Pretreatment of cells with exogenous Na_2S (H_2S-donor) can cause significant DNA damage in cells as shown by gel electrophoresis and comet assays, etc.[2,4,7] Thus, HepG2 and CHO cell models of H_2S-induced DNA damage could be obtained. As shown in **Fig. 3** and **S14**, the fluorescence intensity of **NAN0-N_3** and **NAN6-N_3** in the green channel were significantly lower than that of the control group. This is due to excessive H_2S resulting in DNA damage, which results in release of the probes from the minor groove of DNA, and enables their return to a twisted or folded form (**NAN0-NH_2(T)**, **NAN6-NH_2(F)**), and decreases the fluorescence intensity due to a reduction of the excited state energy. In addition, the fluorescence reduction for **NAN6-N_3** was greater than that of **NAN0-N_3 (Fig. 3** and **S14)**. This was because mtDNA is more vulnerable to damage by H_2S than nDNA [5-7,12] In contrast, the fluorescence intensity of **ND-N_3** was enhanced, since it only interacts with H_2S. These imaging results verified that **NAN0-N_3** and **NAN6-N_3** were suitable for the specific and highly sensitive imaging of nDNA and mtDNA damage induced by H_2S, respectively.

mtDNA can be used as a sensitive marker to distinguish healthy cells from apoptotic cells.[12] Thus, **NAN6-N_3** was anticipated to be a powerful tool for evaluating the degree of apoptosis. Apoptosis of HepG2 cells was induced at different temperatures, and Propidium Iodide (PI) was used as a standardized indicator for the degree of apoptosis. As shown in **Fig. 4a-c**, the green channel (535-575 nm) exhibited a strong fluorescence, while the red channel (600-630 nm) displayed no fluorescence in the control group (*i.e.* healthy cells). With the development of apoptosis, the fluorescence of the green channel decreased significantly, and that of red channel increased. In addition, the same results were obtained in CHO cells (**Fig. S15**). Confirming that, the fluorescence intensity of the green channel decreased significantly with an increase of apoptosis. This is because the damage of mtDNA increases with an increase in the degree of apoptosis. When mtDNA damage increases the amount of binding by **NAN6-N_3** to the minor groove in the non-folded form decreases, and its fluorescence signal intensity decreases. Therefore, **NAN6-N_3** can be used as a highly sensitive tool to help evaluate the degree of cell apoptosis based on the highly sensitive response to H_2S-induced mtDNA damage.

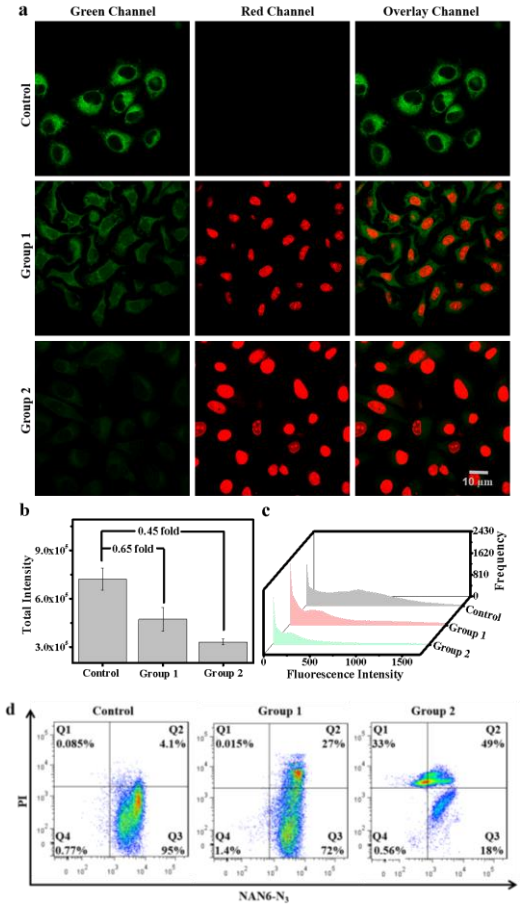

Fig. 4. HepG2 cells staining with **NAN6-N_3** (6.0 μM) and PI (10.0 μM) during cell apoptosis. a, Cell images during cell apoptosis. b, Histogram of the green channel in (a). c, Data for the green channel in (a). d, FCM analyses during cell apoptosis. Control group: untreated cells, healthy cell model. Experimental group 1: the cells were incubated at 56 °C for 4.0 h, early apoptotic cell model. Experimental group 2: the cells were incubated at 65 °C for 4.0 h, late apoptotic cell model. Q1: death. Q2: late apoptosis. Q3: early apoptosis. Q4: healthy cells. **NAN6-N_3**: excitation wavelength = 405 nm, scan range = 535-575 nm (green channel); PI: excitation wavelength = 559

nm, scan range = 600-630 nm (red channel). Incubation time: 30.0 min. Fold: intensity final / intensity at start.

The above results were further verified by flow cytometric (FCM) analysis and high throughput data analysis (**Fig. 4d**). In the control group, 95% of cells in early apoptosis were illuminated by **NAN6-N_3** and exhibited a bright green fluorescence signal (**Fig. S16**). As the degree of apoptosis gradually increased, the number of cells that were illuminated by **NAN6-N_3** decreased significantly (experimental group 1, 72%; experimental group 2, 18%). In addition, the number of cells illuminated by both **NAN6-N_3** and PI increased significantly during apoptosis (control group, 4.1%; experimental group 1, 27%; experimental group 2, 49%), and the green fluorescence signal of **NAN6-N_3** was significantly reduced (**Fig. S16**). This result is consistent with the above cell imaging results. As such, **NAN6-N_3** could evaluate the degree of cell apoptosis through the specific and highly sensitive monitoring of H_2S-induced mtDNA damage in cells.

In summary, two dual-locked probes (**NAN0-N_3** and **NAN6-N_3**) were developed for the specific monitoring of H_2S-induced DNA damage in living cells. Spectral experiments and theoretical calculations confirmed that **NAN0-N_3** and **NAN6-N_3** could strongly bind to DNA through minor groove interactions and cause molecular conformational changes, which inhibited the non-radiative transition energy. Meanwhile, the molecular structure was changed by H_2S (*i.e.* $-N_3$ to $-NH_2$), which increased the density of the intramolecular electron cloud. In this work, ≥ 1.9×10^{-2} mM of H_2S and ≥ 2.2×10^{-2} μg/mL of DNA as dual-keys could activate a highly sensitive fluorescence signal through synergistic changes of the structure and conformation. **NAN0-N_3** and **NAN6-N_3** with different amphiphilicity could specifically monitor H_2S-induced nDNA and mtDNA damage. In addition, **NAN6-N_3** could in real-time evaluate apoptosis by monitoring H_2S-induced mtDNA damage. Therefore, **NAN0-N_3** and **NAN6-N_3** could be used as favorable tools for investigating the pathway of DNA repair and damage caused by H_2S.

This work was supported by the National Natural Science Foundation of China (U21A20314, 22107089, 21722501); T.D.J. wishes to thank the Royal Society for a Wolfson Research Merit Award and the Open Research Fund of the School of Chemistry and Chemical Engineering, Henan Normal University for support (2020ZD01). T. D. J has been appointed as an Outstanding Talent by Henan Normal University. This paper is dedicataed to Xiaojun Peng on the occasion of his 60th birthday.

Conflicts of interest

There are no conflicts to declare.

Notes and references

1. Z. Z. Xie, Y. Liu, J. S. Bian, Hydrogen Sulfide and Cellular Redox Homeostasis, *Oxid. Med. Cell. Longev.*, **2016**, ID: 6043038.
2. R. Shackelford, E. Ozluk, M. Z. Islam, B. Hopper, A. Meram, G. Ghali, C. G. Kevil, Hydrogen sulfide and DNA repair, *Redox Biol.*, **2021**, *38*, 101675-101681.
3. M. S. Attene-Ramos, G. M. Nava, M. G. Muellner, E. D.Wagner, M. J. Plewa, H. R. Gaskins, DNA Damage and Toxicogenomic Analyses of Hydrogen Sulfide in Human Intestinal Epithelial FHs 74 Int Cells, *Environ. Mol. Mutagen.*, **2010**, *51*, 304-314.
4. M. Hoffman, A. Rajapakse, X. Shen, K. S. Gates, Generation of DNA-Damaging Reactive Oxygen Species via the Autoxidation of Hydrogen Sulfide under Physiologically Relevant Conditions: Chemistry Relevant to Both the Genotoxic and Cell Signaling Properties of H_2S. *Chem. Res. Toxicol.*, **2012,** *25*, 1609-1615.
5. D. D. Huang, G. Q. Jing, L. L. Zhang, C. B. Chen, S. H. Zhu, Interplay Among Hydrogen Sulfide, Nitric Oxide, Reactive Oxygen Species, and Mitochondrial DNA Oxidative Damage, *Front. Plant Sci.*, **2021**, *12*, 701681-701691.
6. K. Yaegaki, W. Qian, T. Murata, T. Imai, T. Sato, T. Tanaka, T. Kamoda, Oral malodorous compound causes apoptosis and genomic DNA damage in human gingival fibroblasts, *J Periodont Res*, **2008**, *43*, 391-399.
7. A. Y. Xiao, M. R. Maynard, C. G. Piett, Z. D. Nagel, J. S. Alexander, C. G. Kevil, M. V. Berridgee, C. B. Pattillo, L. R. Rosen, S. Miriyala, L. Harrison, Sodium sulfide selectively induces oxidative stress, DNA damage, and mitochondrial dysfunction and radiosensitizes glioblastoma (GBM) cells, *Redox Bio.*, **2019**, *26*, 101220-101231.
8. X. R. Shi, C. X. Yin, Y. Wen, F. J. Huo, A dual-sites fluorescent probe based on symmetric structure of naphthalimide derivative to detect H_2S, *Dyes Pigments*, **2019**, *165*, 38-43.
9. A. Kafle, S. Bhattarai, J. M. Miller, S. T. Handy, Hydrogen sulfide sensing using an aurone-based fluorescent probe, *RSC Adv.*, **2020**, *10*, 45180-45188.
10. Y. L. Pak, J. Li, K. C. Ko, G. Kim, J. Y. Lee, J. Yoon, Mitochondria-Targeted Reaction-Based Fluorescent Probe for Hydrogen Sulfide, *Anal. Chem.*, **2016**, *88(10)*, 5476-5481.
11. F. P. Kong, X. X. Wang, J. D. Bai, X. Li, C. Yang, Y. Li, K. H. Xu, B. Tang, A double-locked probe for the detection of hydrogen sulfide in a viscous system, *Chem. Commun.*, **2021**, *57*, 6604-6607.
12. Y. F. Wang, H. Y. Niu, K. Wang, G. Wang, J. W. Liu, T. D. James, H. Zhang, mtDNA-Specific Ultrasensitive Near-Infrared Fluorescent Probe Enables the Differentiation of Healthy and Apoptotic Cells, *Anal. Chem.*, **2022**, *94*, 7510-7519.
13. X. Xie, O. Reznichenko, L. Chaput, P. Martin, M. Teulade-Fichou, A. Granzhan, Topology-Selective, Fluorescent "Light-Up" Probes for G-Quadruplex DNA Based on Photoinduced Electron Transfer, *Chem. Eur. J.*, **2018**, *24*, 12638-12651.
14. D. Y. He, L. L. Wang, L. P. Wang, X. Y. Li, Y. P. Xu, Spectroscopic studies on the interactions between novel bisnaphthalimide derivatives and calf thymus DNA, *J. Photoch. Photobio. B.*, **2017**, *166*, 333-340.
15. F. Fueyo-González, M. Fernández-Gutiérrez, D. García-Puentes, A. Orte, J. A. González-Vera, R. Herranz, Naphthalimide-based macrophage nucleus imaging probes, *Eur. J. Med. Chem.*, **2020**, *200*, 112407-112417.
16. K. T. Fam, M. Collot, A. S. Klymchenko, Probing biotin receptors in cancer cells with rationally designed fluorogenic squaraine dimers, *Chem. Sci.,* **2020***, 11,* 8240-8248.
17. M. H. Hu, Molecular engineering of a near-infrared fluorescent ligand for tracking mitochondrial DNA G-quadruplexes, *Anal. Chim. Acta*, **2021**, *1169*, 338600-338604.
18. F. Yang, C. Wang, L. Wang, Z. W. Ye, X. B. Song, Y. Xiao, Hoechst-naphthalimide dyad with dual emissions as specific and ratiometric sensor for nucleus DNA damage, *Chinese Chem. Lett.*, **2017**, *28*, 2019-2022.
19. S. Doose, H. Neuweiler, M. Sauer, Fluorescence Quenching by Photoinduced Electron Transfer: A Reporter for Conformational Dynamics of Macromolecules, *ChemPhysChem*, **2009**, *10*, 1389-1398.
20. J. Furne, A. Saeed, M. D. Levitt, Whole tissue hydrogen sulfide concentrations are orders of magnitude lower than presently accepted values, *Am. J. Physiol-Reg. I.*, **2008**, *295*, R1479-R1485.
21. M. Ishigami, K. Hiraki, K. Umemura, Y. Ogasawara, K. Ishii, H. Kimura, A source of hydrogen sulfide and a mechanism of its release in the brain, *Antioxid. Redox Sign.*, **2009**, *11*, 205-214.

TOC

